Journal of Molecular Liquids 334 (2021) 116016

Contents lists available at ScienceDirect

Journal of Molecular Liquids

journal homepage: www.elsevier.com/locate/molliq

O-nitrobenzyl liposomes with dual-responsive release capabilities for drug delivery

Weihe Yao, Chenyu Liu, Ning Wang, Hengjun Zhou, Farishta Shafiq, Simiao Yu, Weihong Qiao *

State Key Laboratory of Fine Chemicals, School of Chemical Engineering, Dalian University of Technology, Dalian 116024, PR China

ARTICLE INFO

Article history:
Received 7 September 2020
Revised 18 March 2021
Accepted 28 March 2021
Available online 6 April 2021

Keywords:
Anticancer
N, N-NB-DTPA
Photolysis
Dual-responsive
Nitrosobenzaldehyde
DOX

ABSTRACT

To improve the therapeutic efficacy of anticancer drugs and reduce its toxic side effects, we synthesized a series of amphiphilic o-nitrobenzyl molecules 4-(4-N,N,N,N-dicarboxymethyl-diethylenetriamino)acetoxymethyl-3-nitro-N,N-dialk-ylbenzamide (N,N-NB-DTPA) with good photolysis property and acid sensitivity. Simultaneously, N, N-NB-DTPA liposomes composed of the o-nitrobenzyl molecules have good biocompatibility, low hemolysis rate and cytotoxicity, and the drug encapsulation efficiency of the liposomes exceeds 70%. N, N-NB-DTPA-DOX liposomes possess good stability and can keep uniform distribution in PBS solution for 10 days. The drug release rate of these drug-loaded liposomes reaches to the maximums under pH 5.0 and 30 min UV irradiation, revealing pH/UV dual-responsiveness of these drug-loaded liposomes. The low pH makes DOX separate from these drug-loaded liposomes, and the UV irradiation leads to o-nitrobenzyl ester bond cleave, which contribute to accelerate the release of drug from drug-loaded liposomes. Furthermore, N, N-NB-DTPA-DOX liposomes after UV irradiation have better therapeutic effect than single DOX·HCl, which may result from the production of nitrosobenzaldehyde derivatives after UV irradiation.

1. Introduction

Chemotherapy, reported to be the most commonly used treatment for overpowering tumor cells proliferation, can not only kill the tumor cells but also damage normal cells. Compared with the chemotherapy, the drug delivery systems (DDS) with improved drug efficacy and reduced toxicity have become one of the main methods of cancer treatment [1]. DDSs have the ability to accumulate and penetrate the tumor by enhanced tumor permeability and retention (EPR) effect [2]. After endogenous and exogenous stimuli, these DDSs can be triggered to release the drug at specified location and time [3]. Endogenous stimuli are related to tumor microenvironment which includes the acidic pH, overexpressed specific enzymes, overproduced glutathione (GSH) and reactive oxygen species (ROS) [4,5], while exogenous stimuli mainly apply external conditions, such as light, ultrasound, and magnetic fields [2–4].

Owing to the presence of pH gradient from the blood system and normal tissues to tumor tissues, various pH-responsive drug carriers have been reported [6–8]. However, current studies indicates that the drug release rate of single-responsive drug delivery systems is much lower than that of multi-responsive drug delivery systems [9–11]. In exogenous stimuli, light can provide highly accurate external stimuli to activate DDSs composed of photo-responsive molecules, which spatiotemporally controls the release of the payload [12,13]. Among the photoactivable groups, o-nitrobenzyl derivatives (ONB) are commonly used structures for their confirmed photolysis mechanism and excellent photolysis efficiency [13–16]. Mo et al. designed and synthesized a kind of o-nitrobenzyl prodrug which can be degraded to 5-fluorourail by UV irradiation [17]. Zhang et al. developed a kind of o-nitrobenzyl nanoparticles which had high drug loading efficiency and good UV light responsiveness [18]. They also developed a triple-responsive drug delivery platform constructed by o-nitrobenzyl polymer grafted HMSNs which had a better anti-cancer activity *in vitro* under UV irradiation [19]. Furthermore, Pasparakis et al. developed a drug carrier via self-assembly of o-nitrobenzyl block copolymers, and the drug carrier was able to carry out the spatiotemporally controlled drug release at the target site after activation by visible light [20].

The photolysis mechanism of o-nitrobenzyl derivatives is based on the cleavage of o-nitrobenzyl ester bonds into aromatic nitrosobenzaldehyde and carboxylic acid derivatives [21–23]. Previous reports have demonstrated that aromatic nitrosobenzaldehyde is harmful to cells. In brief, the released aromatic

* Corresponding author.
E-mail address: qiaoweihong@dlut.edu.cn (W. Qiao).

https://doi.org/10.1016/j.molliq.2021.116016
0167-7322/

nitrosobenzaldehyde analogs could lead to significant cytotoxicity by inhibiting the expression of poly [ADP-ribose] polymerase [24]. It has been confirmed that iniparib (a nitrobenzene derive) and its nitroso metabolites formed non-specific protein adducts in tumor cells and displayed a certain anticancer effect [25,26]. O'Shaughnessy et al. found that iniparib plus chemotherapy technique were able to improve the clinical benefits and survival of patients with metastatic triple-negative breast cancer without any significant toxic effects [27]. Therefore, the chemotherapy drug combined with the non-toxic o-nitrobenzyl compounds under UV irradiation can produce an enhanced anticancer effect of "0 + 1 > 1".

To this end, we synthesized a series of o-nitrobenzyl amphiphilic molecules (N, N-NB-DTPA) containing a hydrophilic DTPA group (Diethylenetriaminepentaacetic acid, a ligand of nuclear magnetic contrast agent) and a hydrophobic double long-chain o-nitrobenzyl group, and these molecules were able to encapsulate DOX to form drug-loaded liposomes (N, N-NB-DTPA-DOX liposomes). We believed that the photo-responsive drug-loaded liposomes would accumulate at the tumor site by EPR effect. When N, N-NB-DTPA-DOX liposomes enter into endosomes/lysosomes (pH 4.0–6.0), these liposomes will release some anticancer drug DOX in an acidic environment. At the same time, N, N-NB-DTPA-DOX liposomes in endosomes/lysosomes will release more drug molecules and photolysis products after UV irradiation. Finally, the amount of drug will diffuse into the nucleus and inhibit the production of DNA [28], and photolysis products will oxidize the cysteine in ADP-nucleic acid transporter [26]. Therefore, "0 + 1 > 1" effect triggered by UV light results in cell apoptosis (as shown in Scheme 1).

2. Materials and methods

2.1. Materials

Hydrochloric acid (12 mol/L), N, N-dimethylformamide (DMF, AR), chloroform (AR) and methanol (AR) were purchased from Tianjin Kemiou Chemical Reagent Co., Ltd. PBS solution (0.01 M) was prepared by sodium hydrogen phosphate, monobasic potassium phosphate, potassium chloride and sodium chloride in a certain proportion. Sodium hydrogen phosphate (AR), monobasic potassium phosphate (AR), potassium chloride (AR) and sodium chloride (AR) were purchased from Tianjin Bodi Chemical Co., Ltd. Fetal bovine serum (FBS) and Dulbecco's modified Eagle's medium (DMEM), were purchased from Thermo Fisher Scientific. Doxorubicin hydrochloride (DOX·HCl, 98%) was purchased from Dalian Meilun Biotech Co., Ltd. MTT assays were purchased from KGI Biotech. 96-well plates, 24-well plates and cell culture flasks were purchased from Guangzhou Jet Bio-Filtration Co., Ltd.

2.2. Fabrication of N, N-NB-DTPA liposomes

5 mg of N, N-NB-DTPA was dissolved in 1 mL of chloroform and methanol (1:1, v/v) mixed solution in a 25 mL round bottom flask and the solvent was slowly removed to obtain a uniform film by rotary evaporator. The obtained uniform film was put in a vacuum drying oven at 45 °C for overnight to remove residual organic solvent. 5 mL of PBS solution (0.01 M) was added into the uniform film in order to hydrate it for 4 h at 37 °C, followed by sonication of the mixed solution by an ultrasonic signal generator for

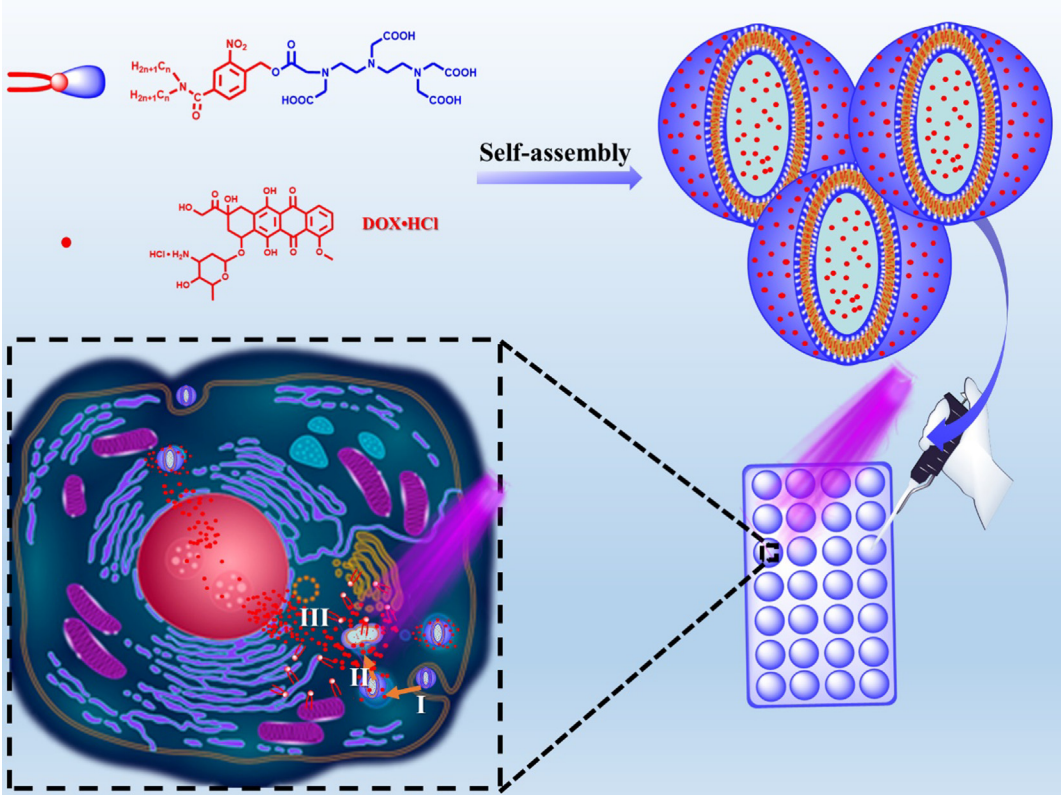

Scheme 1. N, N-NB-DTPA-DOX liposomes were fabricated by self-assembly of N, N-NB-DTPA molecules and an anti-cancer drug DOX· HCl. To verify the enhanced anticancer effect triggered by UV light, these liposomes were co-cultured with MCF-7 cells. Firstly, N, N-NB-DTPA-DOX liposomes taken in by cancer cells will enter into endosomes/lysosomes (pH 4.0–6.0) following with the release of some DOX molecules in the acidic environment. Secondly, N, N-NB-DTPA-DOX liposomes will be broken down with the release of more drug molecules and photolysis products after UV light illumination. Finally, photolysis products will enhance the anticancer effect of drug molecules.

10 min (ultrasound 2 s, intermittent 5 s, 100 W) to fabricate the N, N-NB-DTPA liposomes. The prepared liposomes were used for stability study (the long-term stability and the diluted stability) of liposomes.

0.2 mL of FBS was added to 1.8 mL of solutions containing N, N-NB-DTPA liposomes to study the serum stability of N, N-NB-DTPA liposomes. The prepared liposomes were placed in a constant temperature incubator at 37 °C. The diameter and PDI of N, N-NB-DTPA liposomes were measured by Zetasizer (Malvern Nano S90, Britain) at different time points (0, 7, 24, 51 and 72 h).

2.3. Self-assembly behavior and encapsulation efficiency of N, N-NB-DTPA-DOX liposomes

5 mg of N, N-NB-DTPA was dissolved in 1 mL of chloroform and methanol (1:1, *v/v*) mixed solution in a 25 mL round bottom flask and the solvent was slowly removed from the mixed solution to get a uniform film by rotary evaporator. The product was then dried in a vacuum drying oven at 45 °C for overnight. 5 mL of DOX·HCl solution (1 mg/mL and 0.5 mg/mL) was added into a round bottom flask to hydrate for 4 h at 37 °C, and then the mixed solution was sonicated by an ultrasonic signal generator for 10 min (ultrasound 2 s, intermittent 5 s, 100 W) to form a uniform solution. The resulting mixed solution was then transferred to a dialysis bag (MWCO 3500), followed by immersing it in 500 mL of PBS buffer solution (0.01 M, pH 7.4) along with stirring at a rate of 1000 rpm at room temperature. The process of dialysis was carried out for 8 h while changing the PBS buffer solution every 0.5 h. 20 μL solution from every sample dialysis bag was taken and lyophilized. The lyophilized powder was then dissolved in 5 mL of DMF. The absorption intensity at 486 nm of the DMF solution was measured by ultraviolet spectrophotometer (Agilen, Cary 60), and the concentration of DOX·HCl was determined by the calibration curve ($y = 0.018x - 0.001$, $R^2 = 0.999$, where y is the UV absorption intensity at 486 nm, x is the concentration of DOX·HCl in mg/L).

The drug encapsulation efficiency (DEE) was calculated by the formula as follows:

$$\text{DEE } (\text{wt}\%) = \frac{\text{Mass of loaded drug}}{\text{Mass of drug in feed}} \times 100\%$$

2.4. Hemolysis behavior of N, N-NB-DTPA liposomes

A total of 5 mL fresh blood sample from a healthy volunteer was taken, washed with normal saline and centrifuged at 1500 r/min for 3 min. The above steps were repeated several times until the supernatant was colorless. 400 μL of substrate was diluted to 20 mL with normal saline to form a uniform solution containing 2% red blood cells. 1 mL of normal saline solution containing different concentrations N, N-NB-DTPA and 1 mL of 2% Triton X-100 (TX-100) solution were mixed with 1 mL of 2% red blood cells solution, respectively. The plates were then placed into a constant temperature incubator at 37 °C for 4 h. After 4 h incubation, the mixed red blood cells solution in 24-well plates were centrifuged at 1500 r/min for 3 min. The 100 μL supernatant of different samples was pipetted into a 96-well plate and the absorbance of the 96-well plate was measured by a microplate reader (Multiskan FC, Thermo, USA) at 540 nm.

2.5. pH-responsiveness of N, N-NB-DTPA

2.5.1. Acidic titration

10, 10-NB-DTPA was dissolved in 20 mL NaOH solution to prepare 1 mM aqueous solution of 10, 10-NB-DTPA. The changes in pH and conductivity of 10, 10-NB-DTPA was measured with the addition of 0.01 M HCl solution (0.3 μL/s). The change in transmittance of 10, 10-NB-DTPA in accordance with the change in pH was measured. In the process of acidic titration, the values of pH, conductivity and transmittance were measured by the pH meter model (PHS-3C, Shanghai Hong Yi Instrumentation Co., Ltd), conductivity meter (DDSJ-308A conductivity meter, Shanghai Hong Yi Instrument Co., Ltd.) and a Mettler ToledoT90 instrument, respectively.

2.5.2. Dialysis experiment

The dialysis bags (MWCO 1000) containing 1 mL of 10, 10-NB-DTPA-DOX liposomes solution were placed in 100 mL PBS solutions of different pH (pH 7.4, pH 6.8, and pH 5.0). The diameter and the PDI of the drug-loaded liposomes were measured by Zetasizer after 12 h.

2.6. Photo-responsiveness of N, N-NB-DTPA

2.6.1. Photolysis of N, N-NB-DTPA

1 mg of N, N-NB-DTPA was dissolved in 10 mL $CHCl_3$ in a quartz tube and then irradiated with UV light (365 nm, 60 W) for different time. The distance between the light source (UV 365 nm, 60 W) and samples was fixed at 2 cm. Changes in UV absorption curve, FT-IR spectrum and mass spectrum were measured by UV/VIS/NIR Spectrometer (Lambda 750 S, PerkinElmer Co., Ltd.), Fourier transform-infrared spectrometer (NEXUS, American Thermo Nicolet Co., Ltd.) and accurate mass liquid chromatography time-of-flight mass spectrometer (Accurate-Mass TOF LC/MS 6224, Agilent Technology Co., Ltd.), respectively.

2.6.2. Photolysis behavior of liposomes

Changes in diameter, PDI and Zeta potential of N, N-NB-DTPA liposomes or N, N-NB-DTPA-DOX liposomes in quartz tube were measured by Malvern Zetasizer Nano S90 after UV light irradiation for different time. TEM images of N, N-NB-DTPA liposomes or N, N-NB-DTPA-DOX liposomes before and after UV irradiation were obtained by JOEL JEM-2000EX system. Negative staining samples were prepared with phosphotungstic acid acetate solution (2%).

2.7. Measurement of dual-responsive drug release

In order to determine the accumulative release rate of N, N-NB-DTPA-DOX liposomes, 1 mL of N, N-NB-DTPA-DOX liposomes with different irradiation time (15 min and 30 min) was transferred to dialysis bags (MWCO 3500) followed by immersing them in 100 mL PBS solution with different pH (pH 7.4, 6.8 and 5.0) at 37 °C with a stirring speed of 1000 rpm. Aliquots of 3 mL PBS solution was taken out and then replaced with 3 mL fresh PBS at predetermined intervals. The fluorescence intensity of these aliquots at 590 nm was measured by a fluorescence spectrometer (F7000, Hitachi). According to the doxorubicin standard curve ($y = 133.8x\text{-}0.645$, $R^2 = 0.999$, y is the fluorescence emission intensity at 590 nm, x is the concentration of DOX·HCl), the concentration of DOX was calculated. The cumulative release curve of DOX·HCl was determined as follows:

$$\text{Cumulative release rate of DOX} = \frac{M_t}{M_0} \times 100\%$$

Here, M_t is the cumulative release mass of DOX after time t, and M_0 is the start mass of DOX encapsulated in the liposomes.

2.8. In vitro cytotoxicity of N, N-NB-DTPA liposomes

MCF-7 and HUVEC cells in logarithmic growth stage were seeded in 96-well plates at an approximate cell density of 10^5 cells/mL, followed by placing the plates in 5% CO_2 incubator

at 37 °C for 24 h. The medium was removed and 100 μL of fresh medium containing N, N-NB-DTPA (0.1, 1, 10, 50, 100, 200, 250, 400 and 500 μg/mL) was added. After 24 h incubation, the medium in 96-well plates was removed and each well was washed twice by PBS buffer solution. 150 μL MTT reagent was added to 96-well plates followed by placing the plates in 5% CO_2 incubator at 37 °C for 4 h. The obtained formazan crystals in 96-well plates were dissolved in 150 μL DMSO, and the absorbance at 492 nm was measured by microplate reader after 1 min vibration. Cell viability was determined by the formula $[(A_{sample} - A_0)/(A_{control} - A_0)]$, where $A_{control}$ is the average value of the absorbance from control group, A_{sample} is the average value of the absorbance from cells treated with samples, A_0 is the average value of the absorbance from blank well.

2.9. Photo-induced anticancer activity of N, N-NB-DTPA liposomes and N, N-NB-DTPA-DOX liposomes

MCF-7 cells in logarithmic growth stage were seeded in 96-well plates at an approximate cell density of 10^5 cells/mL followed by putting them in 5% CO_2 incubator at 37 °C.

Non-UV irradiation groups: After the cell density has reached about 80% confluence, the medium was removed and 100 μL fresh medium containing N, N-NB-DTPA and photolysis products of N, N-NB-DTPA (0.1, 1, 10, 20, 40, 50, 60, 80 and 100 μg/mL) or DOX·HCl and N, N-NB-DTPA-DOX (0.1, 1, 5, 10, 15, 20, 25, 30 and 35 μg/mL) was added in each well. After 24 h incubation, the medium in each well was removed and each well was washed twice with PBS solution.

UV irradiation groups: After the cell density has reached about 80% confluence, the medium was then replaced with 100 μL fresh DMEM medium containing N, N-NB-DTPA (0.1, 1, 10, 20, 40, 50, 60, 80 and 100 μg/mL) and N, N-NB-DTPA-DOX (0.1, 1, 5, 10, 15, 20, 25, 30 and 35 μg/mL). After 4 h incubation, 96-well plates were irradiated with UV light (360 nm, 60 W) for 30 min (3 × 10 min). After 20 h incubation, the medium was then removed and each well was washed twice with PBS solution.

150 μL of MTT (0.5 mg/mL, KGI Biotech) reagent was added in the plates. The plates were then placed in CO_2 incubator at 37 °C. After 4 h incubation, the mixed solution was carefully removed in order to obtain formazan crystals. The formazan crystals were dissolved in 150 μL DMSO, and the absorbance of DMSO solution at 492 nm was measured by microplate reader. The cell viability was calculated by the formula $[(A_{sample} - A_0)/(A_{control} - A_0)]$, where $A_{control}$ is the average value of the absorbance from untreated cells, A_{sample} is the average value of the absorbance from cells treated samples, A_0 is the average value of the absorbance from blank well.

3. Results and discussion

3.1. Design and synthesis of photo-cleavable amphiphilic molecule N, N-NB-DTPA

In order to achieve the drug encapsulation and preparation of the photo-controlled release drug, we used o-nitrobenzyl group as a linker of double long hydrophobic carbon chains and hydrophilic DTPA group to synthesize photo-cleavable amphiphilic molecules (N, N-NB-DTPA). The detailed synthesis route of

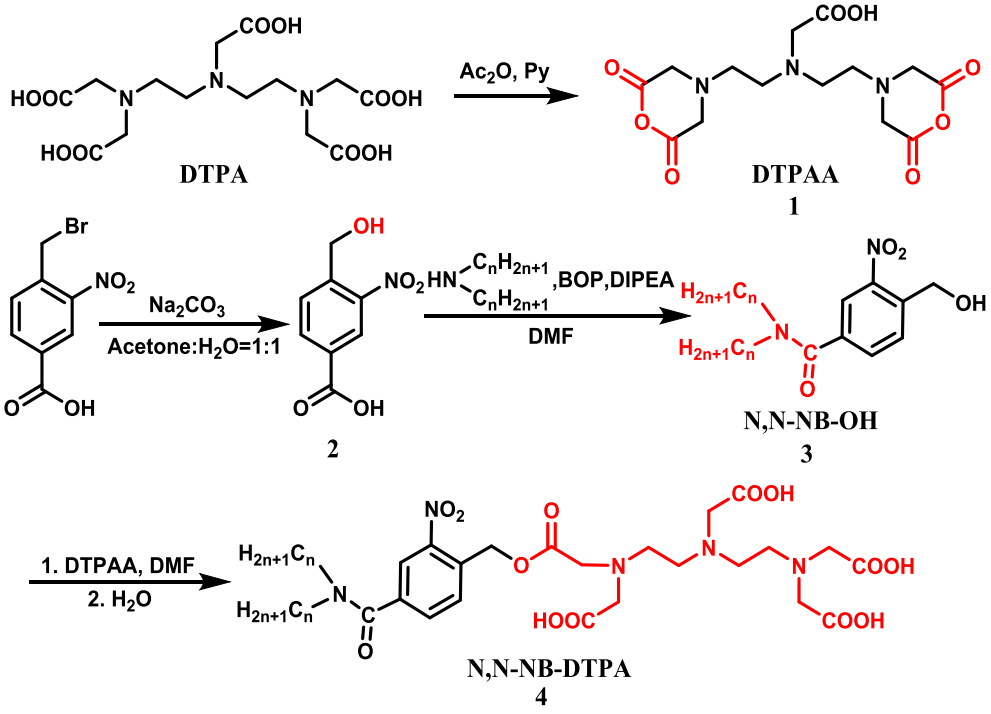

Scheme 2. Synthesis route of photo-cleavable amphiphilic molecule N, N-NB-DTPA.

Table 1
DEE of N, N-NB-DTPA at different mass ratio (drug: lipid).

Mass ratio (D:L)	8,8-NB-DTPA	10, 10-NB-DTPA	12,12-NB-DTPA	14,14-NB-DTPA
DEE (1:1)%	73.8 ± 4.3	76.1 ± 5.1	76.6 ± 4.9	82.6 ± 6.3
DEE (1:2)%	81.2 ± 5.4	85.2 ± 7.1	86.2 ± 9.2	89.7 ± 6.9

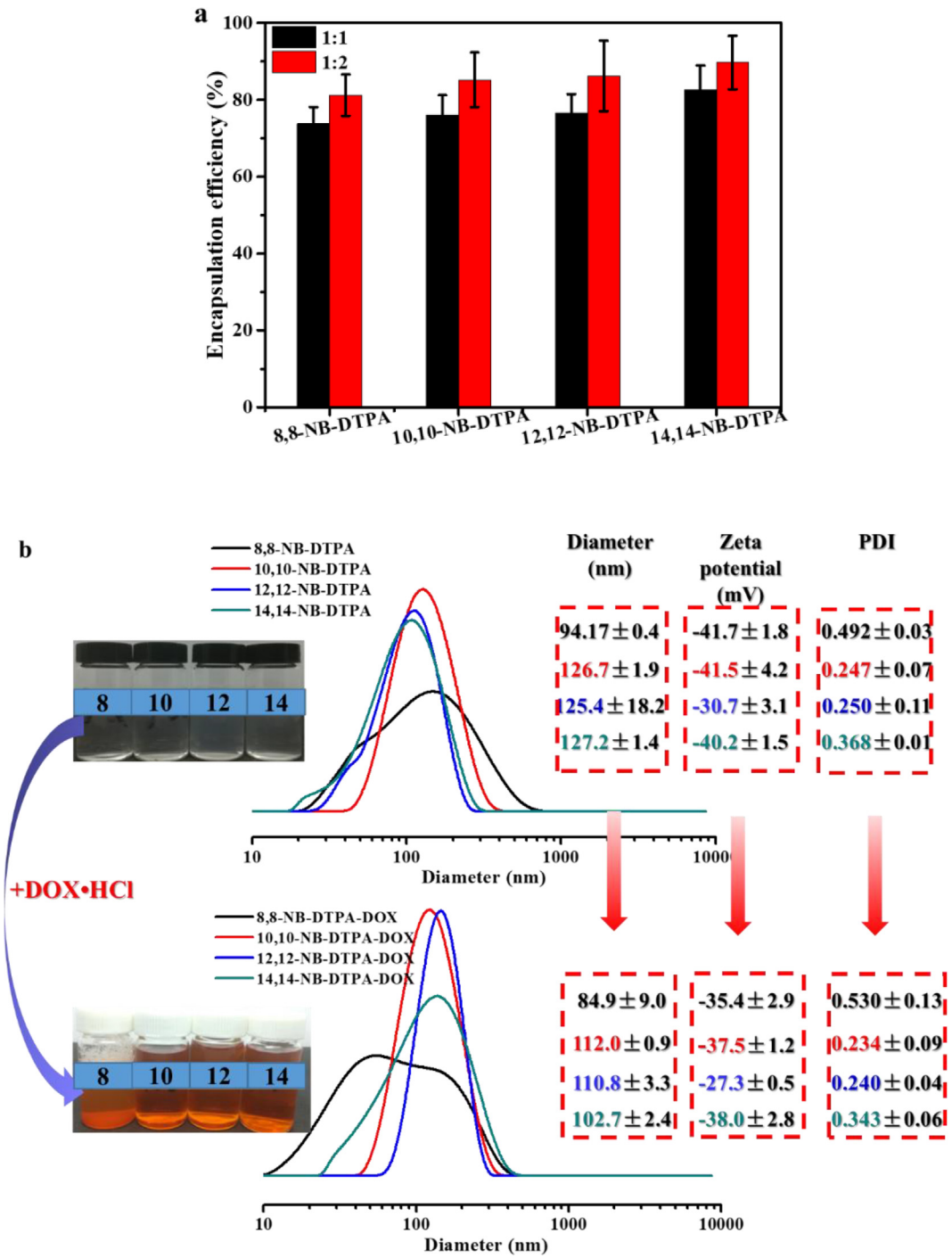

Fig. 1. (a) DEE of N, N-NB-DTPA at different mass ratio (drug:lipid) and (b) changes of state, diameter, Zeta potential and PDI before and after encapsulation of DOX·HCl.

N, N-NB-DTPA is shown in Scheme 2. The detailed synthesis and characterization of products are recorded in supporting information (Section 3.1).

4-(Hydroxymethyl)-3-nitrobenzoic acid prepared by hydrolysis of 4-(bromomethyl)-3-nitrobenzoic acid under reflux in alkaline solution. 4-(hydroxymethyl)-3-nitro-N, N-benzamide (N, N-NB-OH) was synthesized by amidation of 4-(hydroxymethyl)-3-nitrobenzoic acid and secondary amine in presence of BOP and DIPEA. We utilized the high reactivity of hydroxyl and anhydride to synthesize N, N-NB-DTPA. However, the reaction was accompanied by the formation of by-product N, N-NB-DTPA-NB-N, N. To reduce the formation of this by-product, we controlled the ratio and dripping order of hydroxyl and anhydride. The polycarboxyl structure of N, N-NB-DTPA increases the difficulty of purification of the product. After a variety of attempts, we finally chose this ratio (chloroform/methanol/water/acetic acid = 65:25:4:1 v/v) for column chromatography separation. As shown in Fig. S12–S23, the chemical structures of N, N-NB-DTPA were validated by MS, ^{1}H nuclear magnetic resonance spectroscopy (^{1}H NMR) and ^{13}C NMR. Compared with the ^{1}H NMR spectrum of N,N-NB-OH, the methylene (—$C_6H_3CH_2$—) proton signal of N,N-NB-DTPA has shifted from 5.0 ppm to 5.5 ppm. These results suggest that the esterification reaction has occurred. In addition, MS results (shown in Fig. S12, S15, S18 and S21) confirm that the molecular weight of N, N-NB-DTPA (m/z, $[M-H]^-$) is consistent with the calculated value.

3.2. Characterization of N, N-NB-DTPA liposomes

Compared with the traditional surfactant, N, N-NB-DTPA molecules (except for 14, 14-NB-DTPA) exhibited a comparable surface activity (Section 3.2 in supporting information). Herein, water-soluble cationic anticancer drug doxorubicin hydrochloride (DOX·HCl) was selected as the research object in order to study the drug-loading properties. As shown in Table 1 and Fig. 1a, the drug encapsulation efficiencies of N, N-NB-DTPA liposomes exceed 70% which is much higher than the most reported drug delivery systems [29–32]. This higher drug encapsulation efficiencies (DEEs) may be due to the strong electrostatic interaction between the polycarboxylic acid group of N, N-NB-DTPA and the amino-group of DOX·HCl. The inference is further verified by the increase of Zeta potential of DOX-loaded liposomes as shown in (Fig. 2b). In addition, the DEEs of the N, N-NB-DTPA increase with the increase in the length of hydrophobic chain, indicating that the longer hydrophobic chain of N, N-NB-DTPA may form the larger liposome hydrophilic cavity to load more DOX·HCl molecules. However, the diameters of N, N-NB-DTPA liposomes decrease after the encapsulation with DOX·HCl. We speculated that after the encapsulation with DOX·HCl, the electrostatic interaction between the polycarboxylic acid group of N, N-NB-DTPA and the amino-group of DOX·HCl have made the electrostatic repulsion between the molecules in N, N-NB-DTPA liposomes decrease. Furthermore, 10, 10-NB-DTPA liposomes and 12, 12-NB-DTPA liposomes are able to keep uniform size after encapsulation of DOX·HCl by contrast of PDI in Fig. 1b.

3.3. Hemolysis behavior of N, N-NB-DTPA liposomes

In the hemolysis test, we designed to make the solution containing 2% red blood cells divided into positive control group, negative control group and test group. The positive control group was treated with 2% TritonX-100, the negative control group was treated with normal saline and the test group was treated with N, N-NB-DTPA at different concentrations. As seen in the Fig. 2a and b, hemolysis rate of N, N-NB-DTPA is quite low (<5%) except 8, 8-NB-DTPA at 400 μg/mL and 250 μg/mL. As shown in Fig. 2b, compared with the negative control group and the positive control group, the erythrocytes of N, N-NB-DTPA group have no aggregation behavior, indicating good biocompatibility of N, N-NB-DTPA. All these results prove that N, N-NB-DTPA can be applied in drug delivery system at certain concentration range.

3.4. Stability of N, N-NB-DTPA liposomes

The feasibility of N, N-NB-DTPA as a drug-delivery carrier was investigated by measuring the changes in the average diameter of N, N-NB-DTPA liposomes and N, N-NB-DTPA-DOX liposomes at different conditions. Serum stability test was carried out in PBS solution containing 10% FBS at 37 °C. As shown in Fig. 3a and Fig. S25a, N, N-NB-DTPA liposomes can keep stable in PBS solution containing 10% FBS for 72 h. No obvious changes in the average diameters of N, N-NB-DTPA liposomes are observed when the liposomes solution is diluted to 20 times, revealing stability of these liposomes. However, once the liposomes solution is diluted to 50 times, the average diameters and the PDIs of N, N-NB-DTPA liposomes increase sharply (as shown in Fig. 3b and Fig. S25b). In Fig. 3c, the diameters of 10, 10-NB-DTPA and 12,12-NB-DTPA basically have no change in 15 days, while the average diameters of 8,8-NB-DTPA increase and that of 14,14-NB-DTPA decrease. We speculated that 8, 8-NB-DTPA liposomes aggregated to larger liposomes, resulting in an increase of their average diameter. And 14, 14-NB-DTPA liposomes was more prone to form smaller liposomes for low solubility of 14, 14-NB-DTPA molecules, resulting in a decrease of their average diameters. However, the average diameters and the PDIs of N, N-NB-DTPA-DOX liposomes have no significant changes, which may be due to the electrostatic interaction between DOX·HCl and polycarboxylic acid structure of N, N-NB-DTPA (Fig. 3d and Fig. S25d). Especially, 10, 10-NB-DTPA-DOX liposomes and 12, 12-NB-DTPA-DOX liposomes still can keep stable at the 10th day as shown in Fig. 3d and Fig. S25d.

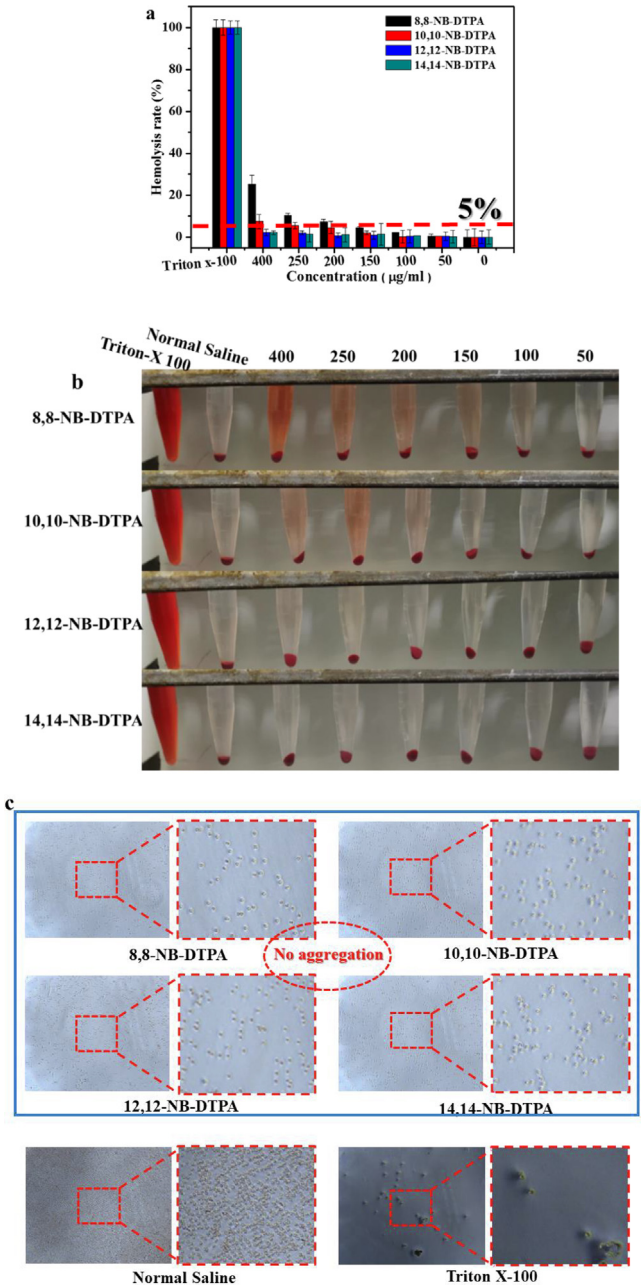

Fig. 2. (a) Hemolysis rate and (b) pictures of N, N-NB-DTPA at different concentration, and (c) microscope image of hemolysis result of N, N-NB-DTPA at high concentration.

3.5. pH-responsiveness of N, N-NB-DTPA

Due to the similarity of the structure of N, N-NB-DTPA, 10, 10-NB-DTPA was chose as the study object for acidic titration. The o-nitrobenzyl ester is prone to cleave once the pH value exceeds 8 [33], so the pH of 1 mM 10, 10-NB-DTPA aqueous

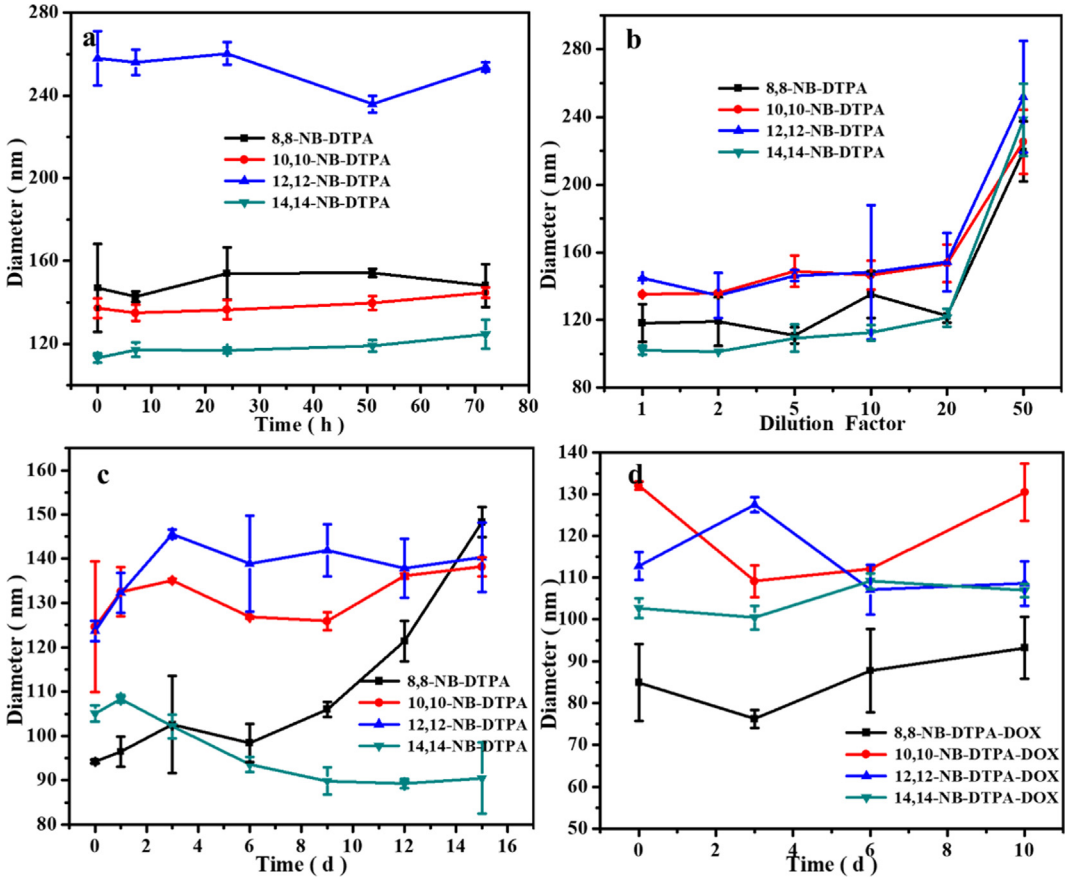

Fig. 3. Diameter of (a) serum stability, (b) dilute stability and (c) long term stability of N, N-NB-DTPA liposomes, and (d) long term stability of N, N-NB-DTPA-DOX liposomes.

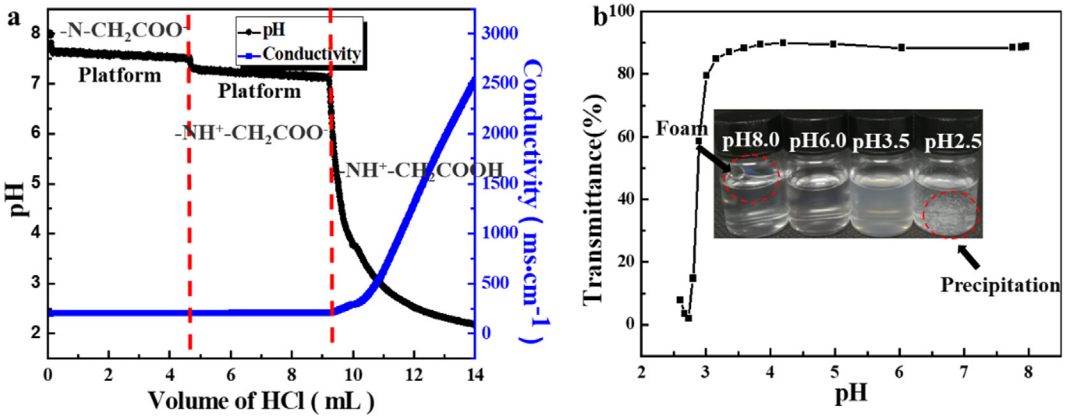

Fig. 4. (a) Acidic titration curves of aqueous 10^{-3} mol/L 10, 10-NB-DTPA, and (b) turbidity of aqueous 10^{-3} mol/L 10, 10-NB-DTPA at different pH conditions.

solution is adjusted to 8, and the state of the solution is shown in Fig. 4b. In the process of the gradual addition of 0.01 M HCl solution to an aqueous solution of 10, 10-NB-DTPA, the changes in the pH and conductivity of the solution are shown in Fig. 4a. We speculated that —N—CH_2COO^- was selectively protonated with H^+ to become —NH^+—CH_2COO^- with appearance of the "platform period" until all —N—CH_2COO^- was converted to —NH^+—CH_2COO^- [34]. Subsequently, —NH^+—CH_2COO^- gradually transferred to poorly water-soluble —NH^+—CH_2COOH with the further addition of H^+, a large amount of white precipitate could be seen in Fig. 4b.

Compared with the diameter of 10, 10-NB-DTPA-DOX liposomes at pH 7.4, the diameter of 10, 10-NB-DTPA-DOX liposomes slightly increase at pH 6.8 and pH 5.0 (in Fig. 5). In acidic environment, the drug molecules are gradually separated from the surface of the liposomes, resulting in an increase in the electrostatic repulsion between the molecules in the liposome, which further leads to an increase of diameter of 10, 10-NB-DTPA-DOX liposomes.

Hence, the pH-responsiveness of 10, 10-NB-DTPA was verified from micro and macro perspectives by combining acidic titration with dialysis experiment.

3.6. Photo-responsiveness of N, N-NB-DTPA

3.6.1. Photocleavage of N, N-NB-DTPA

The cleavage of o-nitrobenzyl ester bond is induced by irradiation with UV light, resulting in the release of drug from the drug-

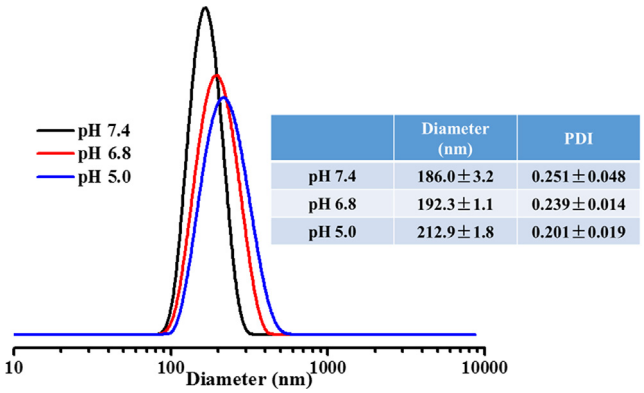

Fig. 5. The diameters and the PDIs of 10, 10-NB-DTPA-DOX liposome at pH 7.4, pH 6.8 and pH 5.0 after 12 h dialysis.

loaded liposomes. Taking 10, 10-NB-DTPA as an example (other N, N-NB-DTPA compounds shown in Fig. S26), the obvious changes can be seen from the UV–Vis spectrum after irradiation at different time as shown in Fig. 6a. As presented in Fig. 6b, the absorption intensity at 270 nm gradually decreases and the absorption intensity at 310 nm gradually increases with the increase of illumination time. Moreover, these two curves have gradually kept their balance after 30 min, which means that the cleavage process of the o-nitrobenzyl ester bond of 10, 10-NB-DTPA has finished after 30 min UV irradiation. In Fig. 6c, the infrared spectrum shows that the —NO_2 stretching vibration of 10, 10-NB-DTPA has disappeared, which further verifies the changes in structure of 10, 10-NB-DTPA after UV illumination. As presented in Fig. 6d, the photolysis products of 10, 10-NB-DTPA are nitrosobenzaldehyde and DTPA, which is consistent with the photodegradation mechanism of o-nitrobenzyl group.

3.6.2. Photolysis behavior of N, N-NB-DTPA liposomes and N, N-NB-DTPA-DOX liposome

To evaluate the photolysis property of N, N-NB-DTPA and N, N-NB-DTPA-DOX liposomes, changes in average diameter, PDI and Zeta potential were measured. As presented in Fig. 7 and Fig. S27, the average diameters of N, N-NB-DTPA and N, N-NB-DTPA-DOX liposomes increased with the increase in UV irradiation

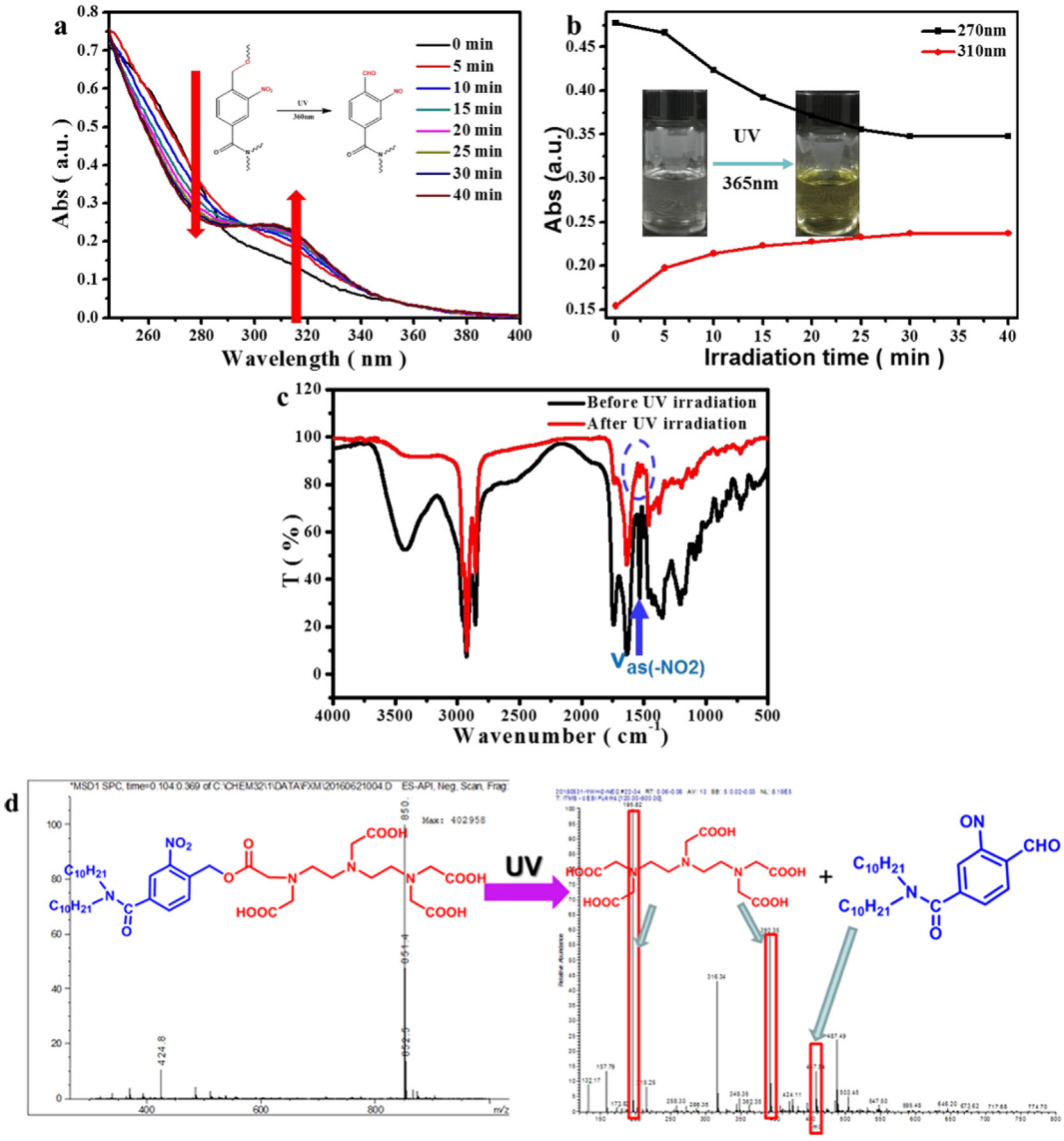

Fig. 6. Changes in (a) UV–Vis spectrum, (b) 270 nm and 310 nm with different UV light irradiation time, changes in (c) IR spectrum and (d) MS of 10, 10-NB-DTPA before and after UV light irradiation.

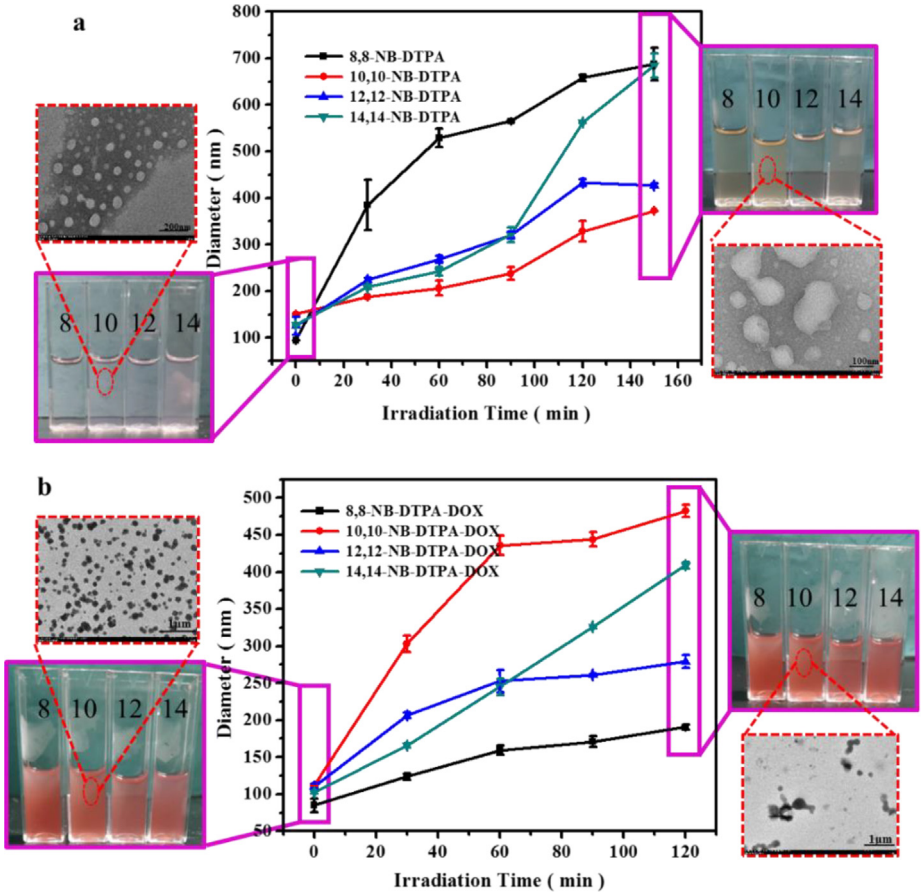

Fig. 7. Changes in average diameter and TEM images of (a) N, N-NB-DTPA liposomes and (b) N, N-NB-DTPA-DOX liposomes with different time UV irradiation.

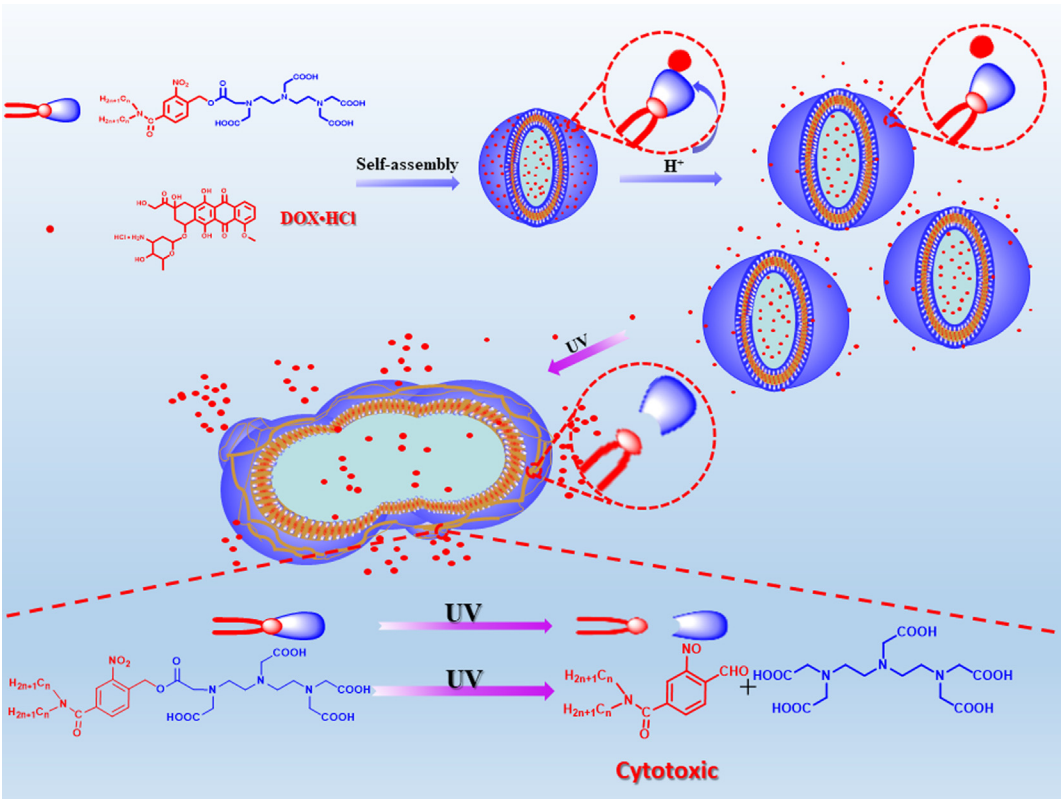

Scheme 3. Mechanism of drug release in acidic environment and with UV irradiation.

time. TEM images in Fig. 7 shows that both 10, 10-NB-DTPA and 10, 10-NB-DTPA-DOX liposomes have uniform spherical structure before UV irradiation (in the top left of the Fig. 7a and b) and irregular shapes (at the bottom right of the Fig. 7a and b) after UV irradiation. To be precise, N, N-NB-DTPA and N, N-NB-DTPA-DOX liposomes aggregate with each other, resulting in an increase of their diameter. O-nitrobenzyl ester bond of N, N-NB-DTPA is cleaved by the UV light, resulting in an increase of their Zeta potential (in Fig. S27). Furthermore, the electrostatic repulsion among the liposomes gradually decreases, which lowers the barrier for membrane fusion and contributes to the drug release. In Scheme 3, the proposed mechanism explains that the increasing number of liposoluble nitrosobenzaldehyde with the increase in UV illumination time makes the pressure change of the loose liposome inside and outside, resulting in the drug release from liposomes [33].

3.7. In vitro drug release of drug-loaded liposomes

In order to simulate the drug release from the drug-loaded liposomes in normal and cancer cells, drug-loaded liposomes were added into dialysis bags (MWCO 3500) to conduct experiments of photo-triggered DOX release. The samples were exposed to UV light for 15 and 30 min, followed by placing them in phosphate buffer solutions having range of pH 5.0, 6.8, and 7.4 at 37 °C, respectively. The fluorescence emission spectrometer with high detection limit was used to detect the fluorescence intensity of DOX released from dialysis bags immersed in different pH solutions. As seen in Fig. 8, the cumulative DOX release rate of N, N-NB-DTPA at pH 5.0 + 30 min condition is higher than the groups of pH 5.0 + 15 min, pH 5.0, 6.8 and 7.4 after 42 h dialysis, and the release rate gradually increases with the decrease in pH value. The drug cumulative release rate in Fig. 8 and Fig. S28 indicates that the acidic environment and the longer UV illumination time can increase the release rate of DOX [29,33]. As shown in Fig. S29, the color of PBS buffer solution deepens gradually with prolonging UV irradiation time and with decrease in pH value, also indicating the release rate of DOX increase. Therefore, N, N-NB-DTPA-DOX liposomes can be used as a potential pH/photo dual-responsive drug delivery system.

3.8. In vitro cytotoxicity of N, N-NB-DTPA liposomes

In order to assess the feasibility of N, N-NB-DTPA molecules as potential drug carriers, we performed cytotoxicity experiment with HUVEC and MCF-7 cells treated with different concentrations of N, N-NB-DTPA (0.1, 1, 10, 50, 100, 200, 250, 400 and 500 μg/mL). After 24 h incubation, the cell viability was obtained by MTT

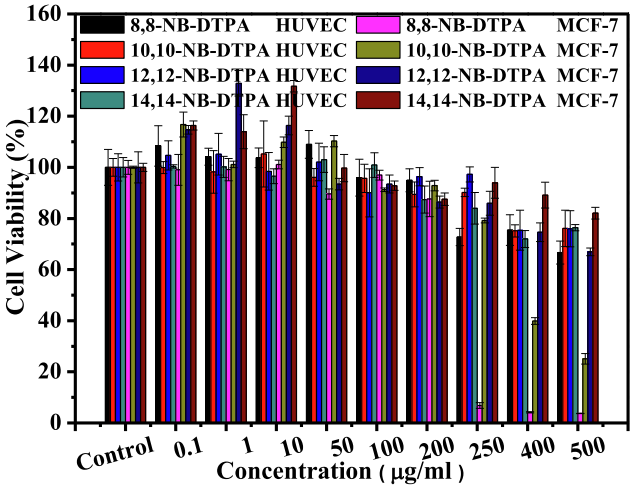

Fig. 9. Cytotoxicity tests of N, N-NB-DTPA (n = 8, 10, 12 and 14) with HUVEC and MCF-7 cells detected by MTT assay.

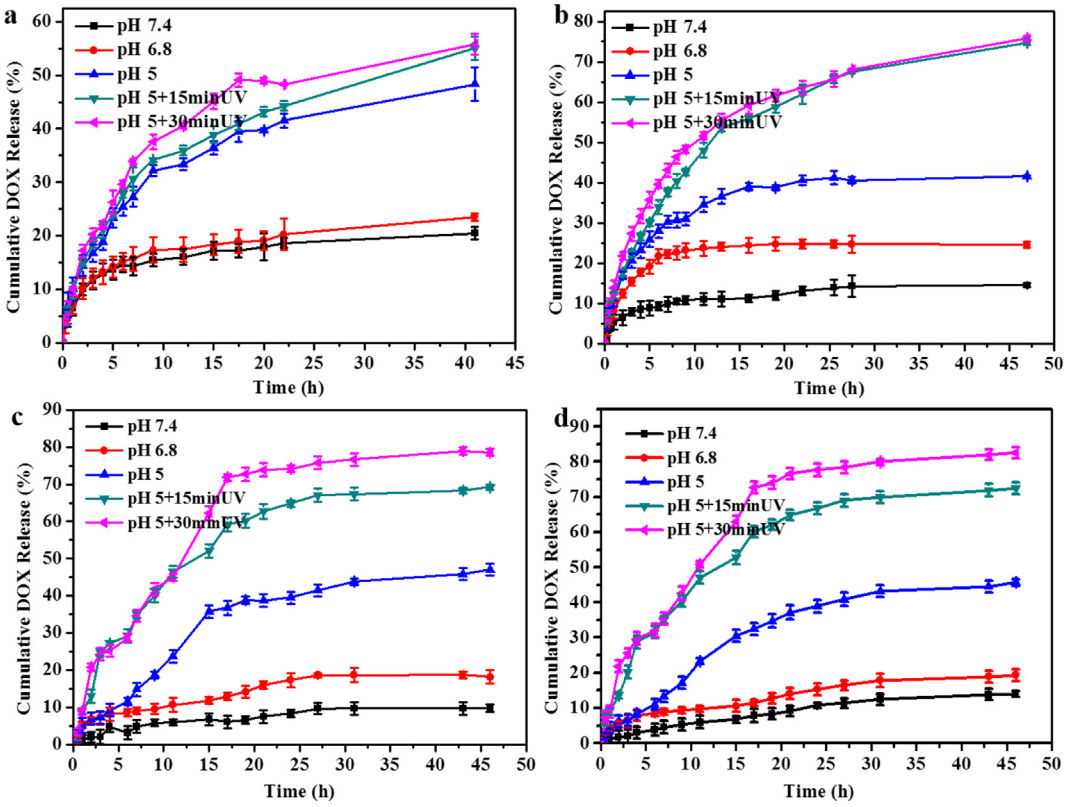

Fig. 8. Cumulative release profiles of DOX-loaded N, N-NB-DTPA liposomes (a) 8,8-NB-DTPA, (b) 10, 10-NB-DTPA, (c) 12,12-NB-DTPA and (d) 14,14-NB-DTPA in 0.01 M PBS buffer at pH 7.4, 6.8, 5.0, pH 5.0 + 15 min UV and pH 5.0 + 30 min UV at 37 °C.

assays. As presented in Fig. 9, when the concentration reaches to 200 μg/mL, the cell viability of HUVEC and MCF-7 cells treated with amphiphilic N, N-NB-DTPA (n = 8, 10, 12, 14) molecules is over 90%. Moreover, when the concentration reaches to 400 μg/mL, the cell viability of MCF-7 cells treated with 14, 14-NB-DTPA is still over 80%. We speculated that this may be related to the good biocompatibility of 14, 14-NB-DTPA molecule. In general, amphiphilic N, N-NB-DTPA molecules could be used as drug carriers owing to their low cytotoxicity.

3.9. Photo-induced anticancer activity of 10, 10-NB-DTPA liposomes

In optimization of experimental conditions (as shown Section 3.3 and Fig. S30 in supporting information), DMEM was selected as the medium, and the illumination time was 3 × 10 min (30 min) for subsequent illumination experiments.

Due to the similar structures and the similar photolysis products of N, N-NB-DTPA, 10, 10-NB-DTPA liposomes were used in study of photo-induced anticancer activity. To prove anticancer effects of the photodegradation products of 10, 10-NB-DTPA, the experiment was divided into three groups [35]: (1) the cells incubated with 10, 10-NB-DTPA liposomes were not subjected to UV irradiation; (2) 10, 10-NB-DTPA liposomes were irradiated by UV light for 30 min before cell incubation; (3) the cells incubated with 10, 10-NB-DTPA liposomes for 4 h were irradiated by UV light for 30 min (3 × 10 min). The cell viability of each group was determined by MTT assay. As shown in Fig. 10a, the cells treated with 10, 10-NB-DTPA liposomes grow well at different concentrations, and the cell viability is still above 100% at 100 μg/mL. In UV pre-

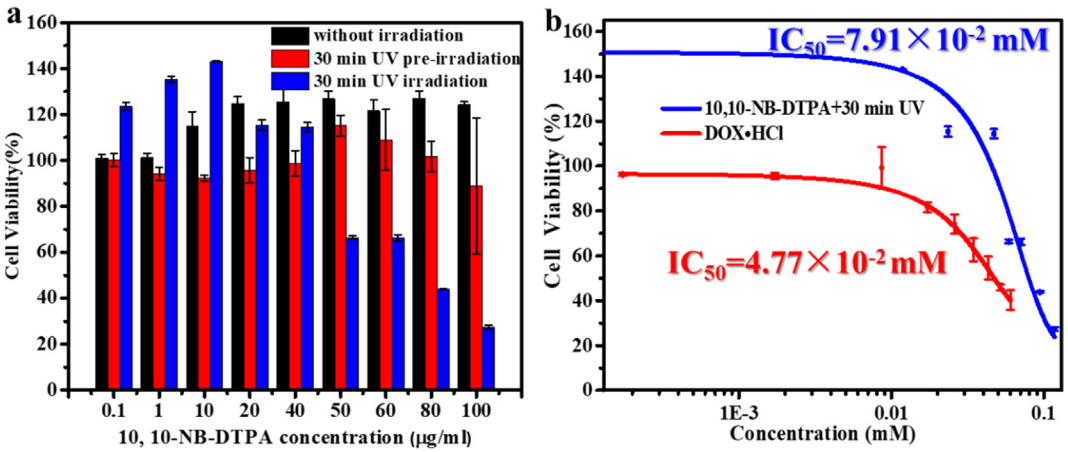

Fig. 10. MTT assay results for 10, 10-NB-DTPA which were incubated with MCF-7 cells. (a) cytotoxicity studies, and (b) IC_{50} of 10, 10-NB-DTPA + 30 min UV and DOX·HCl.

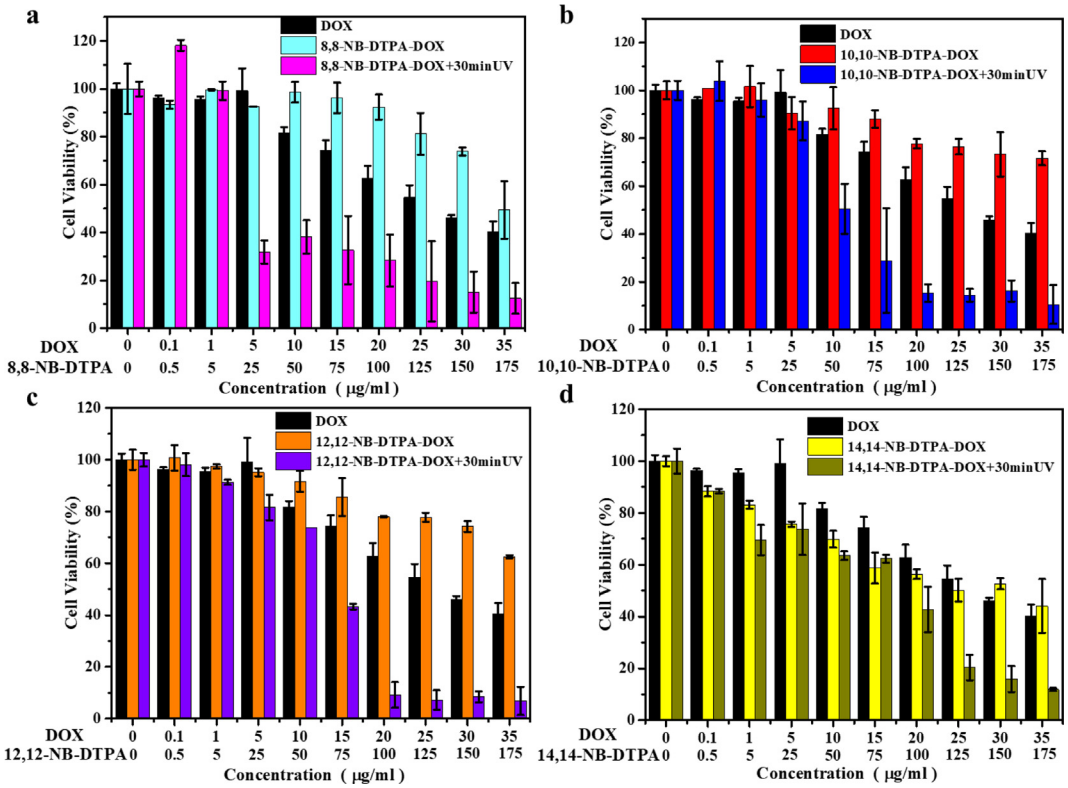

Fig. 11. Photo and drug dual-induced anticancer activity of (a) 8, 8-NB-DTPA-DOX, (b) 10, 10-NB-DTPA-DOX, (c) 12, 12-NB-DTPA-DOX and (d) 14, 14-NB-DTPA-DOX incubated with MCF-7 cells.

irradiation group, the cell viability is 90% at 100 μg/mL. While in UV irradiation group, the cell viability significantly reduces to 65% at 50 μg/mL. Especially, when the concentration reaches to 100 μg/mL, the cell viability is less than 10%. In Fig. 10b, the IC_{50} (IC_{50} = 7.91 × 10^{-2} mM) of MCF-7 cells treated with 10,10-NB-DTPA + 30 min is close to the IC_{50} (IC_{50} = 4.77 × 10^{-2} mM) of MCF-7 cells treated with the anticancer drug DOX·HCl, indicating 10,10-NB-DTPA + 30 min also presents a comparable anticancer activity.

The results of above experiments indicates that the 10, 10-NB-DTPA liposomes have low cytotoxicity, but the products formed by photodegradation significantly inhibit the growth of cancer cells. The cell viability of the pre-irradiation group is significantly different from that of the irradiation group. We speculated that the nitrosobenzene products in pre-irradiation group were either decomposed by cancer cells or combined with extracellular serum protein [35]. While in irradiation group, 10, 10-NB-DTPA liposomes can produce nitrosobenzene products in cancer cells after UV irradiation, which may affect the cell growth. The nitrosobenzene products produced in cancer cells by photolysis enable to oxidize the cysteine in ADP-nucleic acid transporter, which destabilizes the binding of ADP-nucleic acid transporter and Zn^{2+} [26] and inhibits cell proliferation.

3.10. Photo and drug dual-induced anticancer activity of N, N-NB-DTPA-DOX liposomes

N, N-NB-DTPA molecules possess similarity in their structure, so the anticancer activity of N, N-NB-DTPA (n = 8, 12 and 14) liposomes after UV irradiation should be similar with 10, 10-NB-DTPA liposomes. DOX·HCl was loaded in N, N-NB-DTPA liposomes to form N, N-NB-DTPA-DOX liposomes (Drug:Lipid = 1:5). MCF-7 cells were incubated with N, N-NB-DTPA-DOX liposomes for 4 h, which then entered into the cytoplasm and released DOX·HCl molecules into the nucleus (as shown in Fig. S31). Although anticancer activity is not good as the anticancer activity of DOX·HCl (in Fig. 11), N, N-NB-DTPA-DOX liposomes produce anticancer activity when the concentration of DOX reached to 15 μg/mL, which may due to the release of some DOX·HCl molecules from N, N-NB-DTPA-DOX liposomes at acidic environment. The anticancer activity of MCF-7 cells co-incubated with N, N-NB-DTPA-DOX liposomes + UV irradiation is higher than that of DOX·HCl, which may result from the enhanced anticancer effect of "0 + 1 > 1". N, N-NB-DTPA liposomes can be seen as "0" for their low cytotoxicity in a certain concentration range, while DOX·HCl can be seen as "1" for its high anticancer activity at low concentration. Once N, N-NB-DTPA-DOX liposomes (0 + 1) are irradiated by UV light in cancer cell, anticancer activity produced by them is better than the anticancer activity produced by DOX·HCl (>1). Despite the antagonism between DOX·HCl and nitrosobenzaldehyde (in Fig. S32), N, N-NB-DTPA-DOX + UV has more significant cytotoxicity than DOX·HCl alone (in Fig. 11a–d). Apparently, N, N-NB-DTPA-DOX liposomes exhibit the photo and drug dual-induced anticancer activity.

4. Conclusion

In summary, we designed and synthesized a series of amphiphilic o-nitrobenzyl molecules (N, N-NB-DTPA), and prepared a novel pH/photo dual-responsive drug-loaded liposomes. (N, N-NB-DTPA-DOX). N, N-NB-DTPA molecules exhibited high surface activity, low hemolysis and cytotoxicity, and good pH/UV sensitivity. The drug-loading rate of blank liposomes was exceeds 70%, much higher than the most reported drug-loaded carriers. The blank and the drug-loaded liposomes can be stable up to 10 days, while the UV light can make the shape of the blank and drug-loaded liposomes change dramatically. Moreover, acidic environment and UV irradiation time can increase the cumulative release rate of the drug from the drug-loaded liposomes over 60%. We found that the treatment of N, N-NB-DTPA-DOX + UV improved the anticancer effect of DOX·HCl, which may contribute to the oxidation reaction of cysteine and nitrosobenzaldehyde instead of the synergism caused by the DOX·HCl and nitrosobenzaldehyde derivatives. In brief, the enhanced anticancer effect of "0 + 1 > 1" is presented by UV light triggering N, N-NB-DTPA-DOX liposomes. Hence, N, N-NB-DTPA-DOX + UV can be used as a potential therapeutic strategy for cancer therapy.

Declaration of Competing Interest

The authors declare that they have no known competing financial interests or personal relationships that could have appeared to influence the work reported in this paper.

Acknowledgments

This work was supported by International Science & Technology Cooperation Program of China No. 2015DFA41670, China Scholarship Council Talent International Cooperation Project [2019] 13044, the Fundamental Research Funds for the Central Universities DUT19GJ203 and China Postdoctoral Science Foundation 2020M670743.

Appendix A. Supplementary material

Supplementary data to this article can be found online at https://doi.org/10.1016/j.molliq.2021.116016.

References

[1] S. Mura, J. Nicolas, P. Couvreur, Nat. Mater. 12 (2013) 991–1003, https://doi.org/10.1038/nmat3776.
[2] N. Wang, X. Cheng, N. Li, H. Wang, H. Chen, Nanocarriers and their loading strategies, Adv Healthc. Mater. 8 (2019), https://doi.org/10.1002/adhm.201801002.
[3] N. Rahoui, B. Jiang, N. Taloub, Y.D. Huang, Spatio-temporal control strategy of drug delivery systems based nano structures, J. Control. Release. 255 (2017) 176–201, https://doi.org/10.1016/j.jconrel.2017.04.003.
[4] T. Ravula, N.Z. Hardin, S.K. Ramadugu, S.J. Cox, A. Ramamoorthy, Formation of pH-resistant monodispersed polymer-lipid nanodiscs, Angew. Chem. Int. Ed. Engl. 57 (2018) 1342–1345, https://doi.org/10.1002/ange.201712017.
[5] D. Chen, G. Zhang, R. Li, M. Guan, X. Wang, T. Zou, Biodegradable, hydrogen peroxide, and glutathione dual responsive nanoparticles for potential programmable paclitaxel release, J. Am. Chem. Soc. 140 (2018) 7373–7376, https://doi.org/10.1021/jacs.7b12025.
[6] L. Liang, J. Fu, L. Qiu, Design of pH-sensitive nanovesicles via cholesterol analogue incorporation for improving in vivo delivery of chemotherapeutics, ACS Appl. Mater. Interfaces 10 (2018), https://doi.org/10.1021/acsami.7b16891.
[7] Y. Yoshizaki, E. Yuba, N. Sakaguchi, K. Koiwai, A. Harada, K. Kono, pH-sensitive polymer-modified liposome-based immunity-inducing system: Effects of inclusion of cationic lipid and CpG-DNA, Biomaterials (2017) 272–283, https://doi.org/10.1016/j.biomaterials.2017.07.001.
[8] C.H. Heo, M.K. Cho, S. Shin, T.H. Yoo, H.M. Kim, Real-time monitoring of vesicle pH in an endocytic pathway using an EGF-conjugated two-photon probe, Chem. Commun. 52 (2016) 14007–14010, https://doi.org/10.1039/c6cc08036g.
[9] X. Zhao, Z. Wei, Z. Zhao, Y. Miao, Y. Qiu, W. Yang, H. Hou, Design and development of graphene oxide nanoparticle/chitosan hybrids showing pH-sensitive surface charge-reversible ability for efficient intracellular doxorubicin delivery, ACS Appl. Mater. Interfaces 10 (2018) 6608–6617, https://doi.org/10.1021/acsami.7b16910.
[10] R. Zhang, C.N. Leeper, X. Wang, T. White, B. Ulery, Immunomodulatory vasoactive intestinal peptide amphiphile micelles, Biomater. Sci.-UK 6 (2018) 1717, https://doi.org/10.1039/c8bm00466h.
[11] K.T. Hou, T.I. Liu, H.C. Chiu, DOX/ICG-carrying γ-PGA-g-PLGA-based polymeric nanoassemblies for acid-triggered rapid DOX release combined with NIR-activated photothermal effect, Eur. Polym. J. 110 (2019) 283–292, https://doi.org/10.1016/j.eurpolymj.2018.11.038.
[12] B. Razavi, R. Abbaszadeh, M. Salami-Kalajahi, H. Roghani-Mamaqani, Multi-responsive poly(amidoamine)-initiated dendritic-star supramolecular

structures containing UV cross-linkable coumarin groups for smart drug delivery, J. Mol. Liq. (2020), https://doi.org/10.1016/j.molliq.2020.114138.
[13] A. Barhoumi, Q. Lui, D.S. Kohane, Ultraviolet light-mediated drug delivery: Principles, applications, and challenges, J. Control. Release 219 (2015) 31–42, https://doi.org/10.1016/j.jconrel.2015.07.018.
[14] H. Chen, Y. Zhao, Applications of light-responsive systems for cancer theranostics, ACS Appl. Mater. Interface 10 (2018) 21021–21034, https://doi.org/10.1021/acsami.8b01114.
[15] C. Bao, M. Jin, B. Li, Y. Xu, J. Jin, L. Zhu, Long conjugated 2-nitrobenzyl derivative caged anticancer prodrugs with visible light regulated release: preparation and functionalizations, Org. Biomol. Chem. 10 (2012) 5238–5244, https://doi.org/10.1039/c2ob25701g.
[16] L.L. Fedoryshin, A.J. Tavares, E. Petryayeva, Near-infrared-triggered anticancer drug release from upconverting nanoparticles, ACS Appl. Mater. Interface 6 (2014) 13600–13606, https://doi.org/10.1021/am503039f.
[17] S. Mo, Y. Wen, F. Xue, H. Lan, Y. Mao, G. Lv, A novel o-nitrobenzyl-based photocleavable antitumor prodrug with the capability of releasing 5-fluorourail, Sci. Bull. (2016), https://doi.org/10.1007/s11434-016-1010-5.
[18] Y. Zhang, Q. Yin, L. Yin, L. Ma, L. Tang, J. Cheng, Chain-shattering polymeric therapeutics with on-demand drug-release capability, Angew. Chem. Int. Ed. Engl. 52 (2013) 6435–6439, https://doi.org/10.1002/ange.201300497.
[19] Y. Zhang, C.Y. Ang, M. Li, S.Y. Tan, Q. Qu, Z. Luo, Y. Zhao, Polymer-coated hollow mesoporous silica nanoparticles for triple-responsive drug delivery, ACS Appl. Mater. Interface 7 (2015) 18179–18187, https://doi.org/10.1021/acsami.5b05893.
[20] G. Pasparakis, T. Manouras, M. Vamvakaki, P. Argitis, Harnessing photochemical internalization with dual degradable nanoparticles for combinatorial photo–chemotherapy, Nat. Commun. 5 (2014) 36231–36239, https://doi.org/10.1038/ncomms4623.
[21] A. Blanc, C.G. Bochet, Isotope effects in photochemistry: o-nitrobenzyl alcohol derivatives, J. Am. Chem. Soc. 126 (2004) 7174–7175, https://doi.org/10.1021/ja049686b.
[22] K. Petr, S. Tomáš, G.B. Christian, B. Aurélien, G. Richard, R. Marina, Photoremovable protecting groups in chemistry and biology: Reaction mechanisms and efficacy, Chem. Rev. 113 (2013) 119–191, https://doi.org/10.1021/cr300177k.
[23] P. Wang, Photolabile protecting groups: Structure and reactivity, Asian J. Org. Chem. 2 (2013) 452–464, https://doi.org/10.1002/ajoc.201200197.
[24] M.J. Metzger, B.L. Stoddard, R.J. Monnat, PARP-mediated repair, homologous recombination, and back-up non-homologous end joining-like repair of single-strand nicks, DNA Repair 12 (2013) 529–534, https://doi.org/10.1016/j.dnarep.2013.04.004.
[25] J. O'Shaughnessy, L. Schwartzberg, Phase III study of iniparib plus gemcitabine and carboplatin versus gemcitabine and carboplatin in patients with metastatic triple-negative breast cancer, J. Clin. Oncol. 32 (2014) 3840–3847, https://doi.org/10.1200/jco.2014.55.2984.
[26] X. Liu, Iniparib nonselectively modifies cysteine-containing proteins in tumor cells and is not a bona fide PARP inhibitor, Clin. Cancer Res. 18 (2012) 510–523, https://doi.org/10.1158/1078-0432.ccr-11-1973.
[27] J. O'Shaughnessy, Iniparib plus chemotherapy in metastatic triple-negative breast cancer, N. Engl. J. Med. 364 (2011) 205–214, https://doi.org/10.1056/nejmoa1011418.
[28] T.K. Lee, T.C. Lau, I.O. Ng, Doxorubicin-induced apoptosis and chemosensitivity in hepatoma cell lines, Cancer Chemoth. Pharm. 49 (2002) 78–86, https://doi.org/10.1007/s00280-001-0376-4.
[29] X. Zhao, M. Qi, S. Liang, K. Tian, T. Zhou, X. Jia, J. Li, P. Liu, Synthesis of photo- and pH dual-sensitive amphiphilic copolymer PEG43-b-P(AA76-co-NBA35-co-tBA9) and its micellization as leakage-free drug delivery system for UV-triggered intracellular delivery of doxorubicin, ACS Appl. Mater. Interface 8 (2016) 22127–22134, https://doi.org/10.1021/acsami.6b08935.
[30] S. Yang, N. Li, D. Chen, Visible-light degradable polymer coated hollow mesoporous silica nanoparticles for controlled drug release and cell imaging, J. Mater. Chem. B 1 (2013) 4628, https://doi.org/10.1039/c3tb20922a.
[31] M. Hegazy, P. Zhou, G. Wu, Construction of polymer coated core–shell magnetic mesoporous silica nanoparticles with triple responsive drug delivery, Polym. Chem. 8 (2017) 5852–5864, https://doi.org/10.1039/c7py01179b.
[32] X. Xu, S. Lv, W. Can, Curcumin polymer coated, self-fluorescent and stimuli-responsive multifunctional mesoporous silica nanoparticles for drug delivery, Micropor. Mesopor. Mater. 271 (2018) 234–242, https://doi.org/10.1016/j.micromeso.2018.06.009.
[33] C.Y. Liu, K.K. Ewert, N. Wang, Y.L. Li, C.R. Safinya, W.H. Qiao, A multifunctional lipid that forms contrast-agent liposomes with dual-control release capabilities for precise MRI-guided drug delivery, Biomaterials 221 (2019) 119412, https://doi.org/10.1016/j.biomaterials.2019.119412.
[34] J. Lv, W.H. Qiao, Z. Li, Vesicles from pH-regulated reversible gemini amino-acid surfactants as nanocapsules for delivery, Colloid Surf. B 146 (2016) 523–531, https://doi.org/10.1016/j.colsurfb.2016.06.054.
[35] P. Anilkumar, E. Gravel, I. Theodorou, K. Gombert, B. Theze, F. Duconge, E. Doris, Nanometric micelles with photo-triggered cytotoxicity, Adv. Funct. Mater. 24 (2014) 5246–5252, https://doi.org/10.1002/adfm.201400840.